crystals

MDPI

Article

Solvate Formation of Bis(demethoxy)curcumin: Screening and Characterization

Lina Yuan * and Heike Lorenz

Max-Planck-Institut für Dynamik Komplexer Technischer Systeme, 39106 Magdeburg, Germany; lorenz@mpi-magdeburg.mpg.de

* Correspondence: yuan@mpi-magdeburg.mpg.de; Tel.: +49-391-6110-287

Received: 27 September 2018; Accepted: 25 October 2018; Published: 29 October 2018

Abstract: Solvate formation of bis(demethoxy)curcumin (BDMC) was screened. Six solvates were obtained out of the nineteen solvents investigated. In the present work, three solvates, i.e., BDMC-tetrahydrofuran (THF), BDMC-1,4-dioxane (DIO) and BDMC-dimethyl sulfoxide (DMSO), were thoroughly studied. Their desolvation processes were characterized by temperature-resolved powder X-ray diffraction (TR-PXRD), thermogravimetric analysis (TGA) and differential scanning calorimetry (DSC), and hot-stage microscopy (HSM). TR-PXRD shows that all the solvates desolvate as the mother BDMC form and no new polymorph could be obtained. The stoichiometric ratio of solvates was calculated via the mass loss of solvents determined by TGA. The thermal stabilities of the solvates were obtained from DSC data and followed the order: BDMC-DMSO > -THF > -DIO. Moreover, stability performances at ambient storage conditions recorded by PXRD show that BDMC-DMSO was stable over three months.

Keywords: solvates; pharmaceutical compound; bis(demethoxy)curcumin; solid-state; characterization; desolvation

1. Introduction

Solvates are unavoidably formed in the chemical and pharmaceutical industry as compounds are exposed to solvents in many stages, i.e., crystallization [1]. The term solvate refers to a new solid state form, in which the host compound packs together with a solvent [2]. Solvates have several applications: (1) Purification by using the property of solvate formation. Such a purification method was reported for the active pharmaceutical ingredients (APIs) enzalutamide [3] and dirithromycin [4]. (2) Solvates could be optional solid forms of APIs. For example, on the market, trametinib, depagliflozin, cabazitaxel, darunavir, warfarin sodium, indinavir sulfate, and atorvastatin calcium are cases in which the solvated forms are used instead of the unsolvated forms [5]. (3) Solvates can also serve as the precursors of specific polymorphs and sometimes can be the only way to produce the desired forms. Two representative examples are zanoterone [6] and prilocaine hydrochloride [7]. (4) Solvates could be applied to form crystallites with small and homogeneous particle size distribution upon desolvation of stoichiometric solvates. Griseofulvin [8] was reported to apply the solvation and desolvation method to reduce the particle sizes.

Curcuminoids, which can be found exclusively in the roots of turmeric spice *Curcuma longa*, possess various medicinal activities, such as anti-inflammatory, antioxidant, antiproliferative, antiangiogenic, and anticancer [9–13]. Commercially available curcuminoids consist of three main components: curcumin (CUR), demethoxycurcumin (DMC) and bis(demethoxy)curcumin (BDMC) [14–16]. The three components are structurally similar (Figure 1), which makes the separation and purification quite challenging [17,18]. The method of using the property of solvate formation might be helpful for the separation. In addition, specific polymorphs might be obtained upon the desolvation.

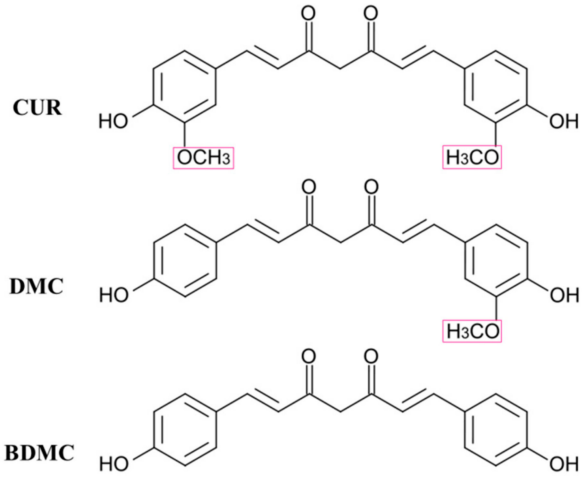

Figure 1. Molecular structures of curcumin (CUR), demethoxycurcumin (DMC), and bis(demethoxy)curcumin (BDMC).

Among the three curcuminoids, CUR is often considered to be responsible for the medical properties, but recent studies report that BDMC has certain better properties than CUR [19,20]. Moreover, literature data reveals increasing interest in the BDMC solvate formation. Karlsen et al. [21] unveiled a BDMC monohydrate from ethanol. Solvates crystallized from methanol and from isopropanol were found by Tønnesen [22] and Kasai et al. [23], respectively. Solvates recrystallized from ethyl acetate and acetonitrile were described in a patent [24]. Often the stability of solvates is low. In some cases, they desolvate as soon as they are removed from the mother liquor [25,26]. Apparently, the most desirable solid form to develop is the stable crystalline form, as it has the lowest tendency to transform during scale-up, processing, formulation or storage [27]. Therefore, it is essential to evaluate the stability of solvates [28,29]. However, for the above-reported BDMC solvates, no information regarding their stabilities is indicated. Therefore, it is of prime importance to have thorough investigations of the solvate formation of BDMC.

This work focuses on the investigation of solvate formation of BDMC and the evaluation of their stabilities. Nineteen solvents were chosen for screening, and the obtained solvates were comprehensively characterized by powder X-ray diffraction (PXRD), temperature-resolved powder X-ray diffraction (TR-PXRD), thermal analyses (TGA/DSC), and hot-stage microscopy (HSM). Moreover, the binding energy (enthalpy of desolvation) of the solvates was estimated and thus an indication of their stabilities was acquired.

2. Materials and Methods

2.1. Materials

Bis(demethoxy)curcumin (BDMC) (CAS No. 24939-16-0), purity higher than 98%, was obtained from TCI (Tokyo, Japan) and used as received. Solvents of HPLC grade were purchased from commercial suppliers.

2.2. Preparation of the Powdered Solvates

Saturated solutions were prepared in 5-mL glass vials by dissolving BDMC in the solvents at temperatures close to the boiling point of their respective solvents. The saturated solutions were then filtered while hot using 0.45-μm membrane filters. The solutions were cooled to room temperature until the solid solvates crystallized. In the case of no appearance of solids, the solutions were kept at −20 °C in the refrigerator to induce the crystallization.

2.3. Powder X-ray Diffraction (PXRD)

X-ray powder data were collected on an X'Pert Pro diffractometer (PANalytical GmbH, Kassel, Germany) using Cu-Kα radiation (λ = 1.5418 Å). Samples were scanned in a 2θ range of 3° to 40° with a step size of 0.0017° and a counting time of 50 s per step. Samples were measured at ambient temperature directly after being removed from the mother liquors.

2.4. Temperature-Resolved Powder X-ray Diffraction (TR-PXRD)

To apply a linear increase of temperature and compare TR-PXRD results with other techniques (DSC and HSM), freshly prepared samples were heated to the desired temperature at 5 °C·min^{-1} on a separated Linkam THMS 600 heating plate and then measured with PXRD at ambient temperature.

2.5. Thermal Analyses

Thermogravimetric/differential scanning calorimetry (TGA/DSC) analyses were performed on a Netzsch STA 449 C instrument. Samples were put in a 25-µL aluminum crucible and heated at a rate of 5 °C·min^{-1}. Helium was used as the purge gas. The chemical nature of the released gases during heating was identified by using a Netzsch QMS 403 C Mass Spectrometer (MS) coupled with the TGA/DSC apparatus.

2.6. Hot-Stage Microscopy (HSM)

HSM observations were performed on a Nikon Eclipse LV100 microscope (maximum magnification 1000×) with a CCD camera and coupled with a THMS 600 hot-stage setup (Linkam, Waterfield, UK), which allows an accurate control of the sample temperature (± 1 °C). Selected single crystals were loaded on a quartz cell with a cylindrical geometry (d = 13 mm, h = 1.3 mm). Images were recorded in the temperature range of 30 °C and 100 °C with a heating rate of 5 °C·min^{-1}.

3. Results and Discussion

3.1. Solvate Screening

When choosing the solvents for screening, less attention was paid to the aspect of the pharmaceutical acceptability, since polymorphs could also be produced from the desolvation of the solvates. Nineteen commonly used solvents in the crystallization process were chosen. Powdered samples were prepared and PXRD was used to check the forms obtained.

The complete screening results are summarized in Table 1. It can be seen that six solvates were found out of the nineteen solvents investigated, i.e., BDMC-ACET (acetone), -MeOH (methanol), -THF (tetrahydrofuran), -IPA (isopropanol), -DIO (1,4-dioxane), and -DMSO (dimethyl sulfoxide). PXRD patterns of the six solvates are shown in Figure 2. BDMC, recrystallized from methanol and isopropanol, formed solvates as reported by Tønnesen [22] and Kasai [23]. In our work, no hydrate or solvate was obtained by recrystallization from ethanol, but a BDMC monohydrate was obtained in the work of Karlsen et al. [21]. However, the purity of the ethanol used was not reported, whereas in our work, ethanol of purity higher than 99.5% (absolute ethanol) was used. No solvate was formed from ethyl acetate and acetonitrile in our work as compared to the solvate formation reported in the patent [24]. The reason for the inconsistency of the two results could be due to the instability of the solvates. As soon as the solvates were isolated from the mother liquors, the desolvation occurred rapidly and the solvates could not be detected by PXRD.

Additionally, information of the solubility of BDMC in solvents is given in Table 1. BDMC is more soluble in the polar solvents (except water) compared to the nonpolar solvents. This rough estimation of solubility could provide information when performing purification experiments of curcuminoids by recrystallization from solvents [17,30].

In this work, the three new solvates obtained from tetrahydrofuran, 1,4-dioxane and dimethyl sulfoxide, i.e., BDMC-THF, BDMC-DIO and BDMC-DMSO, were thoroughly investigated. Solvates obtained from acetone, methanol and isopropanol were detailed in our other report.

Table 1. Solvate screening results for BDMC.

Solvent	Boiling Point of Solvent/°C	Relative Polarity of Solvent	Solvate Formation	Solubility of BDMC	PXRD
Dichloromethane	40			Low-	
Acetone (ACET)	56	0.355	Yes	High+	√
Methyl Acetate	57	0.253	No	High	√
Chloroform	61	0.259		Low	
Methanol (MeOH)	65	0.762	Yes	High+	√
Tetrahydrofuran (THF)	66	0.207	Yes	High+	√
n-Hexane	68	0.009		Low-	
Ethyl Acetate	77	0.228	No	High+	√
Ethanol	78	0.654	No	High+	√
Benzene	80	0.111		Low	
Acetonitrile	82	0.460	No	High-	√
Isopropanol (IPA)	83	0.546	Yes	High+	√
n-Heptane	98	0.012		Low-	
Water	100	1.000		No	
1,4-Dioxane (DIO)	101	0.164	Yes	High	√
Toluene	111	0.099		Low	
Acetic Acid	118	0.648	No	Normal	√
Butyl Acetate	126		No	High-	√
Dimethyl Sulfoxide (DMSO)	189	0.444	Yes	High++	√

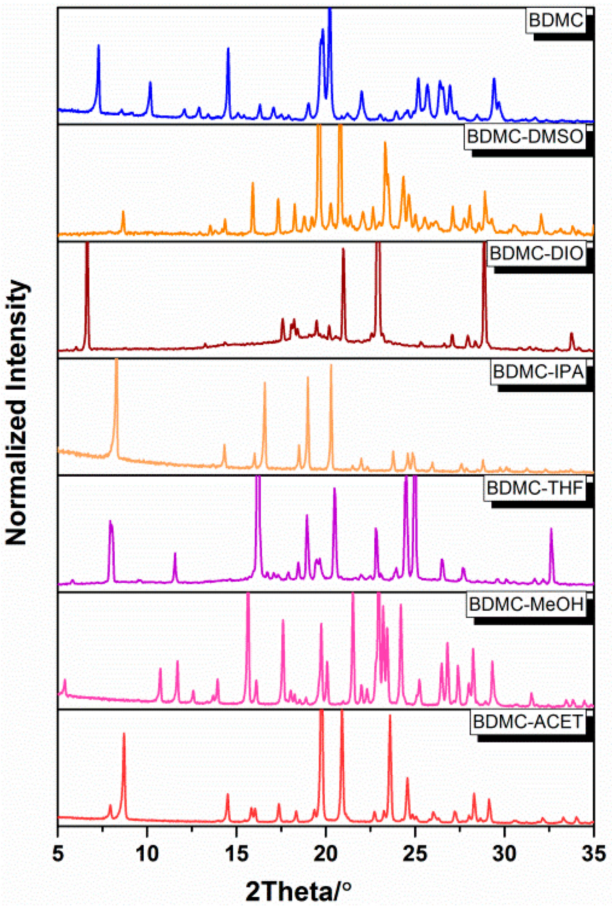

Figure 2. Powder X-ray diffraction (PXRD) patterns of the BDMC solvates: BDMC-ACET (acetone), -MeOH (methanol), -THF (tetrahydrofuran), -IPA (isopropanol), -DIO (1,4-dioxane), -DMSO (dimethyl sulfoxide) with pattern of the pure BDMC at the top for comparison.

3.2. Desolvation of BDMC Solvates

Desolvation of BDMC-THF, -DIO and -DMSO was thoroughly investigated by temperature-resolved powder X-ray diffraction (TR-PXRD), thermogravimetric analysis and differential scanning calorimetry (TGA/DSC), and hot-stage microscopy (HSM).

3.2.1. Temperature-Resolved Powder X-ray Diffraction

TR-PXRD patterns were collected from ambient temperature at 5 °C·min^{-1} to follow the desolvation process of BDMC solvates. The results are shown in Figure 3. To have a clear comparison between various temperatures, only the data collected in the 2θ range of 5° and 35° are shown. For BDMC-THF (Figure 3a), characteristic peaks of BDMC at 2θ = 7.3° and 14.5° appeared in the temperature range of 30 °C to 50 °C and were accompanied by the disappearance of characteristic peaks of BDMC-THF at 2θ = 8.0°, 16.2° and 24.5°. At 60 °C, the desolvation process completed and no further changes occurred until 95 °C. For BDMC-DIO (Figure 3b), characteristic peaks of BDMC at 2θ = 7.3° and 14.5° appeared at 60 °C and were followed by the disappearances of characteristic peaks of BDMC-DIO at 2θ = 6.6°, 21°, 22.9°, and 28.9°. The desolvation process finished at 90 °C. For BDMC-DMSO (Figure 3c), the characteristic peaks of BDMC appeared at 70 °C and the desolvation process continued. At 110 °C, traces of BDMC-DMSO still existed (peak at 2θ = 20.8°). For the three solvates, no new polymorph of BDMC was discovered after the desolvation, thus providing no pathway to produce new polymorphs.

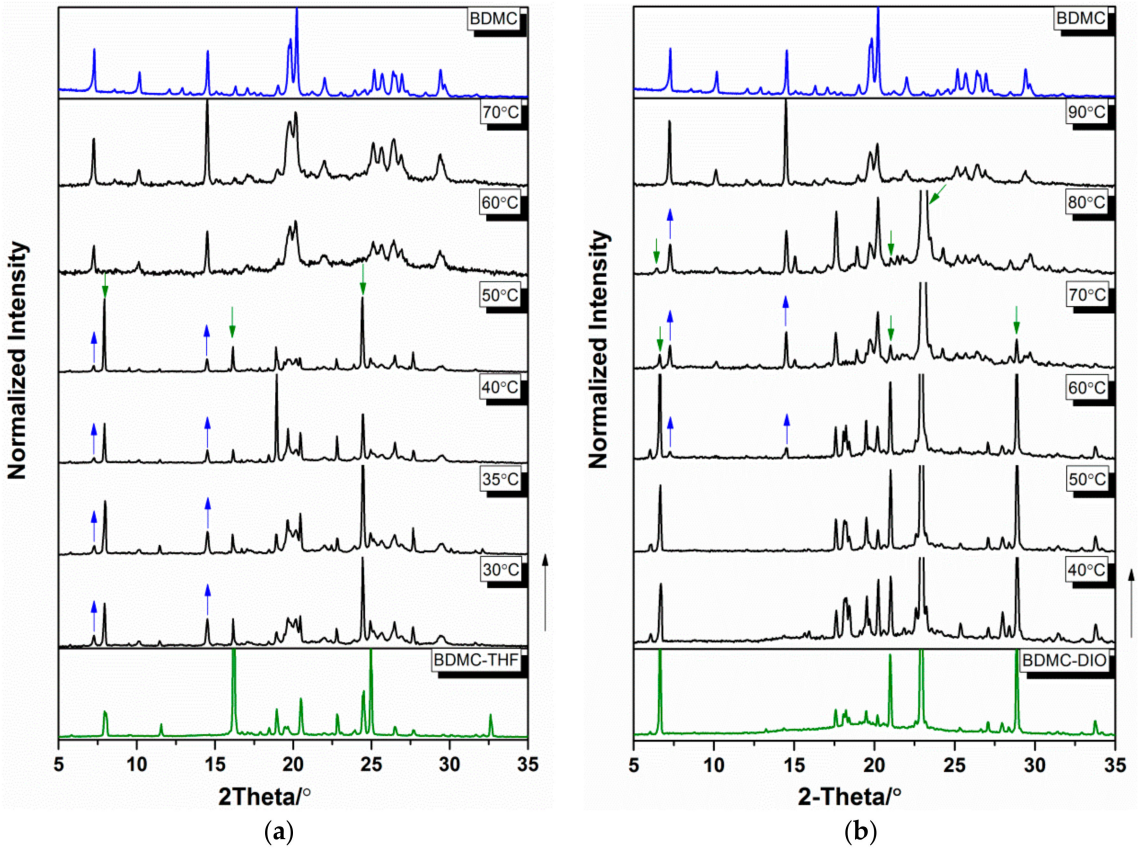

Figure 3. *Cont.*

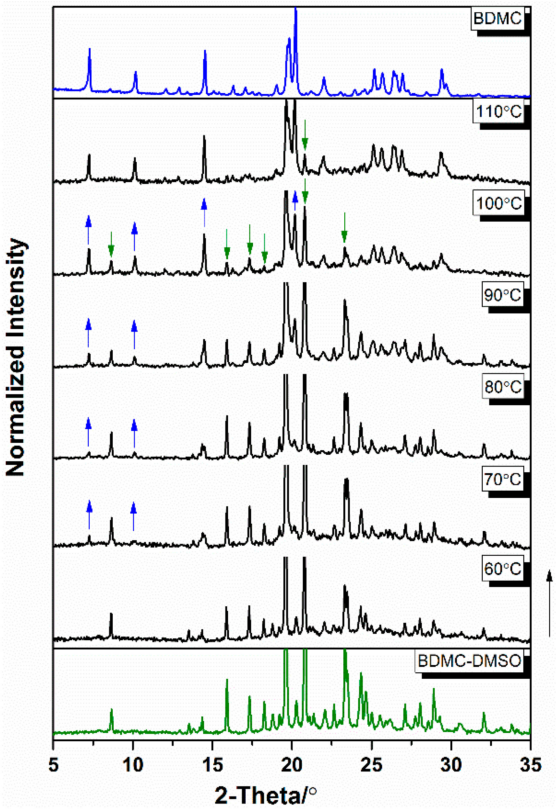

Figure 3. Temperature-resolved powder X-ray diffraction (TR-PXRD) patterns of (**a**) BDMC-THF (tetrahydrofuran), (**b**) BDMC-DIO (1,4-dioxane), and (**c**) BDMC-DMSO (dimethyl sulfoxide). Appearance and disappearance of the characteristic peaks of BDMC and its solvates are indicated by the arrows.

3.2.2. Thermogravimetric Analysis and Differential Scanning Calorimetry

TGA/DSC analyses were used for the characterization of the thermal behavior of BDMC solvates. The thermograms are shown in Figure 4. Characteristic endothermic peaks, corresponding to the desolvation process and the melting of the desolvated BDMC, could be clearly recognized. However, the degradation of BDMC occurred upon the melting process, which is indicated by the mass loss starting simultaneously with melting and the sudden jump of the DSC curve to exothermal conditions.

The three BDMC solvates exhibited very interesting thermal behavior upon desolvation. For BDMC-THF and BDMC-DIO, two distinguishable desolvation steps were observed, which might indicate the existence of intermediate solvates. No indication of the supposed solvates was given by TR-PXRD measurements. The reason could be that the supposed solvates exist in a narrow temperature range and cannot be distinguished by PXRD. Therefore, the resolution of the crystal structures is necessary to elucidate this issue. For BDMC-THF, the first step represents a mass loss of 4.57%, which corresponds to approximately one-quarter of THF. The second step characterizes a mass loss of 3.47% of THF, which is less than one-quarter. Therefore, the ratio of BDMC:THF is 1:0.5 and a hemisolvate is expected. BDMC-DIO shows a continuous two-step mass loss providing a BDMC:DIO ratio of 1:1.5. BDMC-DMSO was measured in a different way. The solvate was preheated to 50 °C to ensure the loss of solvent that was trapped in the interstices of crystals. The ratio of BDMC:DMSO is estimated at 1:0.7. A monosolvate of BDMC-DMSO might be expected.

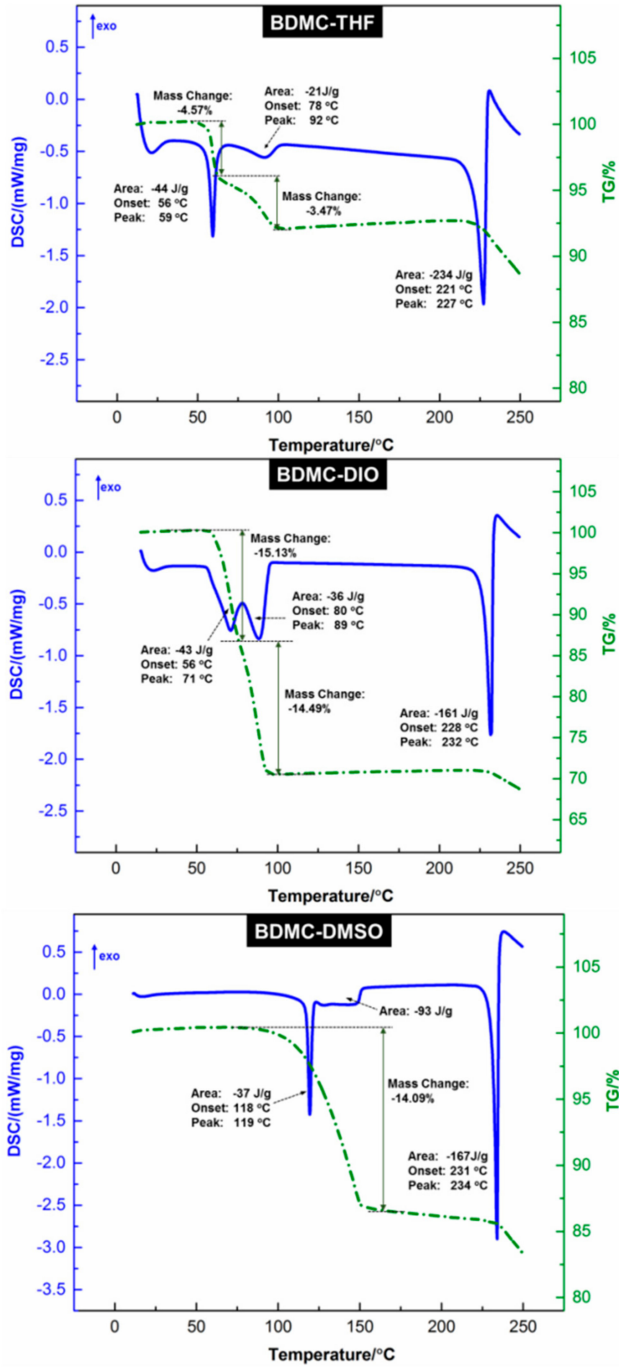

Figure 4. Thermogravimetric analysis and differential scanning calorimetry (TGA/DSC) thermograms that depict the thermal behavior with desolvation and melting of BDMC-THF, BDMC-DIO, and BDMC-DMSO, respectively (heating rate of 5 °C·min^{-1}).

3.2.3. Estimation of the Binding Energy

The quantitative estimation of the stability of solvates can be established by determining the binding energy (enthalpy of desolvation). The binding energy per mole of the bound solvent ΔH_S (J·mol^{-1}) can be calculated from the experimental enthalpy of desolvation $\Delta H_{S,exp}$ (J·g^{-1}) per gram of solvate, the percentage of mass loss Δm_s% and the molecular mass of the solvent M_S, as given in Equation (1) [31–33]:

$$\Delta H_S = \left[\left(\Delta H_{S,exp} \times 100 \right) / \Delta m_S\% \right] \times M_S \quad (1)$$

To determine whether the solvent molecules are strongly or loosely bounded in the host lattice, the calculated binding energy was compared to the corresponding enthalpy of vaporization of the pure solvents (summarized in Table 2) [34]. The calculated values of BDMC-THF and BDMC- DMSO exceed the enthalpy of vaporization of the pure solvents, which indicates that the solvates are firmly bonded. Contrarily, in the BDMC-DIO, interactions were found to be less strong, indicated by the low binding energy value that is clearly below the enthalpy of vaporization of the pure solvent.

Table 2. Thermal data and mass loss of the desolvation of BDMC solvates.

BDMC Solvate	Boiling Point of Pure Solvent/°C	Desolvation Temperature/°C (DSC)		Mass Loss Upon Desolvation (%) via TGA	Enthalpy of Desolvation byDSC/J·g^{-1}	Calculated Enthalpy of Desolvation (BindingEnergy)/kJ·mol^{-1}	Enthalpy of Vaporization of Pure Solvent at 25°C/kJ·mol^{-1}	Ratio of BDMC:Solvent
		Onset T/°C	Peak T/°C					
THF	66	56 78	59 92	4.57 3.47	65	58.21	32.47	1:0.5
DIO	101	56 80	71 89	15.13 14.49	79	23.47	38.60	1:1.5
DMSO	189	118	119	14.09	37	71.97	52.90	1:1

3.2.4. Hot-Stage Microscopy

Despite numerous attempts, no single crystals of sufficient quality could be produced for the three solvates. Nevertheless, for BDMC-THF, a big crystal suitable for visual observations through hot-stage microscopy (HSM) but having an overlapping with another crystal was obtained. The same heating rate (0.5 °C·min^{-1}) was applied as for TR-PXRD and TGA/DSC measurements. Pictures recorded at various temperatures are presented in Figure 5. BDMC-THF forms plate-like crystalline form. Traces of desolvated BDMC were observed at 44 °C under polarized light (black spots) and the highest rate of desolvation occurred in the temperature range of 46 °C to 48 °C. At 52 °C, the desolvation process completed and was accompanied by the total loss of the birefringence.

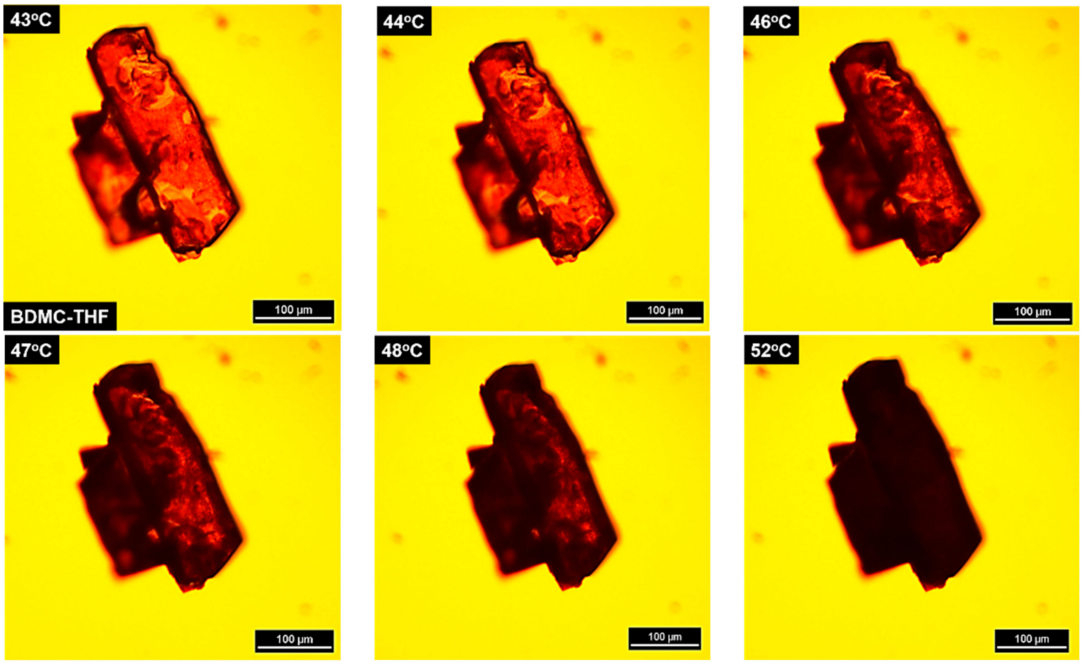

Figure 5. Hot-stage microscopy (HSM) observation on the desolvation process of BDMC-THF with increasing temperature at 5 °C·min^{-1}.

3.3. Comparison of the Desolvation Temperatures of BDMC Solvates

Desolvation temperatures of the three solvates measured by TR-PXRD, DSC and HSM are summarized in Table 3. The start and end temperatures were determined as the onset and peak

temperature by DSC, and by TR-PXRD and HSM as the temperature range in which the desolvation occurred most prominently. Obviously, compared to BDMC-THF and BDMC-DIO, the higher desolvation temperature of BDMC-DMSO indicates that it is the most thermally stable solvated form of BDMC. For the three solvates, it could be seen that the end temperatures of the desolvation measured by TR-PXRD are always lower than the end temperatures measured by DSC. Different temperatures obtained from TR-PXRD and DSC can be attributed to the different conditions of measurements, i.e., samples from TR-PXRD were measured in open and ambient environments, while samples from DSC were measured under nearly closed condition (pierced crucible) and helium flux atmosphere.

Table 3. Desolvation temperatures of BDMC solvates determined by TR-PXRD, DSC and HSM.

BDMC Solvate	TR-PXRD		DSC		HSM	
	Start T (°C)	End T (°C)	Start T (°C)	End T (°C)	Start T (°C)	End T (°C)
THF	40	50	56	92	46	48
DIO	70	80	56	89	/	/
DMSO	90	100	118	/	/	/

3.4. Stability of BDMC Solvates at Ambient Conditions

The stability of the three solvates at ambient conditions was monitored by PXRD. BDMC-THF started to desolvate shortly after the exposure to ambient conditions. The desolvation of BDMC-DIO started after one day of storing. No desolvation occurred for BDMC-DMSO after three months of storing at ambient conditions. Therefore, the order of the stability for BDMC solvates at ambient conditions could be envisaged as: BDMC-DMSO > -DIO > -THF.

4. Conclusions

The present work aims at searching for new solvates of BDMC and characterizing their stabilities. Nineteen solvents were used for the solvate screening and six of them were found to form solvates with BDMC under the conditions applied. BDMC-THF, BDMC-DIO and BDMC-DMSO were thoroughly investigated in this work by TR-PXRD, TGA/DSC and HSM. The desolvation behavior of the prepared solvates is shown to be complex from TGA/DSC results. BDMC forms a hemisolvate with THF, a monosolvate with DMSO, and BDMC-DIO contains 1.5 mole dioxane. The possible existence of intermediate solvates requires further studies. The stability investigations show that BDMC-DMSO is the most stable form upon exposure to thermal treatment and ambient atmosphere. Single crystal XRD was not feasible as no high-quality single crystal could be obtained. Therefore, further investigations on the crystal structures are essential.

Author Contributions: Conceptualization, L.Y. and H.L.; Investigation, L.Y.; Methodology, L.Y.; Project administration, L.Y. and H.L.; Resources, H.L.; Writing—original draft, L.Y.; Writing—review & editing, H.L.

Funding: This research received no external funding.

Acknowledgments: The authors thank Gérard Coquerel for providing the opportunity to use analytical set-ups in the SMS lab in Rouen and Nicolas Couvrat for his assistance in measuring the TGA/DSC data.

Conflicts of Interest: The authors declare no conflict of interest.

References

1. Surov, A.O.; Solanko, K.A.; Bond, A.D.; Bauer-Brandl, A.; Perlovich, G.L. Diversity of felodipine solvates: Structure and physicochemical properties. *CrystEngComm* **2015**, *17*, 4089–4097. [CrossRef]
2. Griesser, U.J. The importance of solvates. In *Polymorphism: In the Pharmaceutical Industry*; Hilfiker, R., Ed.; WILEY-VCH Verlag GmbH & Co. KGaA: Weinheim, Germany, 2006; pp. 211–233. ISBN 3-527-31146-7.
3. Maini, L.; Braga, D.; Farinella, F.; Melotto, E.; Verzini, M.; Brescello, R.; Michieletto, I.; Munari, I. Crystal forms of enzalutamide and a crystal engineering route to drug purification. *Cryst. Growth Des.* **2018**, *18*, 3774–3780. [CrossRef]

4. Wirth, D.D.; Stephenson, G.A. Purification of dirithromycin. Impurity reduction and polymorph manipulation. *Org. Process Res. Dev.* **1997**, *1*, 55–60. [CrossRef]
5. Tieger, E.; Kiss, V.; Pokol, G.; Finta, Z.; Rohlíček, J.; Skořepová, E.; Dušeke, M. Rationalization of the formation and stability of bosutinib solvated forms. *CrystEngComm* **2016**, *18*, 9260–9274. [CrossRef]
6. Rocco, W.L.; Morphet, C.; Laughlin, S.M. Solid-state characterization of zanoterone. *Int. J. Pharm.* **1995**, *122*, 17–25. [CrossRef]
7. Schmidt, A.C.; Niederwanger, V.; Griesser, U.J. Solid-state forms of prilocaine hydrochloride. *J. Therm. Anal. Calorim.* **2004**, *77*, 639–652. [CrossRef]
8. Sekiguchi, K.; Horikoshi, I.; Himuro, I. Studies on the method of size reduction of medicinal compounds. III. Size reduction of griseofulvin by solvation and desolvation method using chloroform. *Chem. Pharm. Bull.* **1968**, *16*, 2495–2502. [CrossRef] [PubMed]
9. Mahady, G.B.; Pendland, S.L.; Yun, G.; Lu, Z.Z. Turmeric (*Curcuma longa*) and curcumin inhibit the growth of *Helicobacter pylori*, A group 1 carcinogen. *Anticancer Res.* **2002**, *22*, 4179–4181. [PubMed]
10. Sugiyama, Y.; Kawakishi, S.; Osawa, T. Involvement of the beta-diketone moiety in the antioxidative mechanism of tetrahydrocurcumin. *Biochem. Pharmacol.* **1996**, *52*, 519–525. [CrossRef]
11. Sanphui, P.; Goud, N.R.; Khandavilli, U.B.R.; Bhanoth, S.; Nangia, A. New polymorphs of curcumin. *Chem. Commun.* **2011**, *47*, 5013–5015. [CrossRef] [PubMed]
12. Jordan, W.C.; Drew, C.R. Curcumin—A natural herb with anti-HIV activity. *J. Natl. Med. Assoc.* **1996**, *88*, 333–335. [PubMed]
13. Sanphui, P.; Goud, N.R.; Khandavilli, U.B.R.; Nangia, A. Fast dissolving curcumin cocrystals. *Cryst. Growth Des.* **2011**, *11*, 4135–4145. [CrossRef]
14. Poornima, B.; Prasad, K.V.S.R.G.; Bharathi, K. Evaluation of solid-state forms of curcuminoids. *Int. J. Pharm. Sci. Res.* **2016**, *7*, 4035–4044. [CrossRef]
15. Sandur, S.K.; Pandey, M.K.; Sung, B.; Ahn, K.S.; Murakami, A.; Sethi, G.; Limtrakul, P.; Badmaev, V.; Aggarwal, B.B. Curcumin, demethoxycurcumin, bisdemethoxycurcumin, tetrahydrocurcumin and turmerones differentially regulate anti-inflammatory and anti-proliferative responses through a ROS-independent mechanism. *Carcinogenesis* **2007**, *28*, 1765–1773. [CrossRef] [PubMed]
16. Suresh, K.; Nangia, A. Curcumin: Pharmaceutical solids as a platform to improve solubility and bioavailability. *CrystEngComm* **2018**, *20*, 3277–3296. [CrossRef]
17. Ukrainczyk, M.; Hodnett, B.K.; Rasmuson, A.C. Process parameters in the purification of curcumin by cooling crystallization. *Org. Process Res. Dev.* **2016**, *20*, 1593–1602. [CrossRef]
18. Péret-Almeida, L.; Cherubino, A.P.F.; Alves, R.J.; Dufossé, L.; Glória, M.B.A. Separation and determination of the physico-chemical characteristics of curcumin, demethoxycurcumin and bisdemethoxycurcumin. *Food Res. Int.* **2005**, *38*, 1039–1044. [CrossRef]
19. Ruby, A.J.; Kuttan, G.; Babu, K.D.; Rajasekharan, K.N.; Kuttan, R. Anti-tumour and antioxidant activity of natural curcuminoids. *Cancer Lett.* **1995**, *94*, 79–83. [CrossRef]
20. Syu, W.-J.; Shen, C.-C.; Don, M.-J.; Ou, J.-C.; Lee, G.-H.; Sun, C.-M. Cytotoxicity of curcuminoids and some novel compounds from *Curcuma zedoaria*. *J. Nat. Prod.* **1998**, *61*, 1531–1534. [CrossRef] [PubMed]
21. Karlsen, J.; Mostad, A.; Tønnesen, H.H. Structural studies of curcuminoids. VI. Crystal structure of 1,7-bis(4-hydroxyphenyl)-1,6-heptadiene-3,5-dione hydrate. *Acta Chem. Scand. B* **1988**, *42*, 23–27. [CrossRef]
22. Tønnesen, H.H.; Karlsen, J.; Mostad, A.; Pedersen, U.; Rasmussen, P.B.; Lawesson, S.-O. Structural studies of curcuminoids. II. Crystal structure of 1,7-bis(4-hydroxyphenyl)-1,6-heptadiene-3,5-dione methanol complex. *Acta Chem. Scand. B* **1983**, *37*, 179–185. [CrossRef]
23. Kasai, K.; Saito, A.; Sato, S. Crystal structure and pseudopolymorphism of bisdemethoxycurcumin-alcohol solvates. *Bull. Miyagi Univ. Educ.* **2017**, *51*, 83–88.
24. Chava, S.; Gorantla, S.R.A.; Muppidi, V.K. Solid forms of curcumin and derivatives thereof. WO2015052568A2, 16 April 2015.
25. Tauvel, G.; Sanselme, M.; Coste-Leconte, S.; Petit, S.; Coquerel, G. Structural studies of several solvated potassium salts of tenatoprazole crystallizing as conglomerates. *J. Mol. Struct.* **2009**, *936*, 60–66. [CrossRef]
26. Braun, D.E.; Kahlenberg, V.; Gelbrich, T.; Ludescher, J.; Griesser, U.J. Solid state characterisation of four solvates of R-cinacalcet hydrochloride. *CrystEngComm* **2008**, *10*, 1617–1625. [CrossRef]
27. Ahuja, D.; Bannigan, P.; Rasmuson, A.C. Study of three solvates of sulfamethazine. *CrystEngComm* **2017**, *19*, 6481–6488. [CrossRef]

28. Bērziņš, A.; Skarbulis, E.; Rekis, T.; Actiņš, A. On the formation of droperidol solvates: Characterization of structure and properties. *Cryst. Growth Des.* **2014**, *14*, 2654–2664. [CrossRef]
29. Zvoníček, V.; Skořepová, E.; Dušek, M.; Babor, M.; Žvátora, P.; Šoóš, M. First crystal structures of pharmaceutical ibrutinib: Systematic solvate screening and characterization. *Cryst. Growth Des.* **2017**, *17*, 3116–3127. [CrossRef]
30. Heffernan, C.; Ukrainczyk, M.; Gamidi, R.K.; Hodnett, B.K.; Rasmuson, A.C. Extraction and purification of curcuminoids from crude curcumin by a combination of crystallization and chromatography. *Org. Process Res. Dev.* **2017**, *21*, 821–826. [CrossRef]
31. Caira, M.R.; Bettinetti, G.; Sorrenti, M.; Catenacci, L. Relationships between structural and thermal properties of anhydrous and solvated crystalline forms of brodimoprim. *J. Pharm. Sci.* **2007**, *96*, 996–1007. [CrossRef] [PubMed]
32. Chadha, R.; Arora, P.; Kaur, R.; Saini, A.; Singla, M.L.; Jain, D.S. Characterization of solvatomorphs of methotrexate using thermoanalytical and other techniques. *Acta Pharm.* **2009**, *59*, 245–257. [CrossRef] [PubMed]
33. Chadha, R.; Arora, P.; Saini, A.; Jain, D.S. Solvated crystalline forms of nevirapine: Thermoanalytical and spectroscopic studies. *AAPS PharmSciTech.* **2010**, *11*, 1328–1339. [CrossRef] [PubMed]
34. Karan, M.; Chadha, R.; Chadha, K.; Arora, P. Identification, characterization and evaluation of crystal forms of quinine sulphate. *Pharmacol. Pharm.* **2012**, *3*, 129–138. [CrossRef]